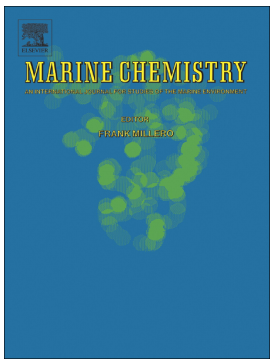

Insoluble prokaryotic membrane lipids in continental shelf sediments offshore Cape Town: Implications for organic matter preservation

Lidia Chaves Torres, Leanne A. Melbourne, Maria T. Hernandez-Sanchez, Gordon N. Inglis, Richard D. Pancost

PII: S0304-4203(17)30080-4
DOI: doi:10.1016/j.marchem.2017.10.003
Reference: MARCHE 3506

To appear in: *Marine Chemistry*

Received date: 6 March 2017
Revised date: 5 October 2017
Accepted date: 14 October 2017

Please cite this article as: Lidia Chaves Torres, Leanne A. Melbourne, Maria T. Hernandez-Sanchez, Gordon N. Inglis, Richard D. Pancost , Insoluble prokaryotic membrane lipids in continental shelf sediments offshore Cape Town: Implications for organic matter preservation. The address for the corresponding author was captured as affiliation for all authors. Please check if appropriate. Marche(2017), doi:10.1016/j.marchem.2017.10.003

Insoluble prokaryotic membrane lipids in continental shelf sediments offshore Cape Town: Implications for organic matter preservation

Lidia Chaves Torres[a,b*], Leanne A. Melbourne[a,b], Maria T. Hernandez-Sanchez[a,b], Gordon N. Inglis[a,b], Richard D. Pancost[a,b]

[a]Organic Geochemistry Unit, School of Chemistry, University of Bristol, Cantock's Close, Bristol BS8 1TS, UK

[b]Cabot Institute, University of Bristol, Bristol BS8 1UJ, UK

*Corresponding author:

chylc@my.bristol.ac.uk

Keywords: marine sediments, insoluble organic matter, selective chemical degradation carbonates, GDGTs, TEX_{86}

Abstract

The largest organic carbon (OC) reservoir on Earth is in the geosphere, mainly comprising insoluble organic matter (IOM). IOM formation, therefore, plays an important role in the short and long-term carbon cycle, carbon bioavailability and formation of source rocks. To explore the mechanism of insolubilization of organic matter (OM), we have analysed soluble and IOM fractions of continental shelf marine sediments. We have applied sequential solvent-extractions followed by a selective chemical degradation of the post-extraction residue, specifically targeting prokaryotic membrane lipids (branched fatty acids – FAs, hopanoids, archaeol and glycerol dialkyl glycerol tetraethers – GDGTs). Up to 80% of prokaryotic membrane lipids are not solvent-extractable, and we observe compound-specific differences in partitioning between soluble and IOM fractions. Based on these observations, we propose a variety of mechanisms for the incorporation of prokaryotic lipids into IOM in marine sediments: First, OM association with authigenic carbonates; second, cross-linking via esterification reactions with time, which could be particularly relevant for FAs; third, competition between reactivity and loss of polar head groups, the latter rendering the OM less susceptible to incorporation; and finally, inherent solvent-insolubility of some lipids associated with prokaryotic cells.

1. Introduction

The largest OC reservoir on Earth is in the geosphere, occurring mainly as kerogen-like materials (15,000 Eg C; Berger et al., 1989; Ronov et al., 1990; Schidlowski, 2001; Harvey, 2006), and its formation plays an important role in the short and long-term carbon cycle and the formation of source rocks. The mechanisms by which OC leaks from the fast carbon cycle into the geosphere have been the focus of many studies over the past decades (e.g. Philp and Calvin, 1976; Harvey et al., 1983; Largeau et al., 1984; Tissot and Welte, 1984; Largeau et al., 1986; Derenne et al., 1988; Tegelaar et al., 1989b; Sinninghe Damsté and de Leeuw, 1990; Hatcher et al., 1996; Garcette-Lepecq et al., 2004; Versteegh et al., 2004; de Leeuw, 2007; Gupta et al., 2007b). Moreover, a variety of techniques have been used to elucidate the structure of OC in the geosphere, which occurs mostly as IOM (see review on kerogen-like materials, Rullkötter and Michaelis, 1990; and more recently, Vandenbroucke and Largeau, 2007).

Recently, in Chaves Torres and Pancost (2016), the use of prokaryotic membrane lipids as tracers for the processes that form IOM in the geosphere was investigated. This built on previous work that had shown how a diverse range of prokaryotic lipids, including branched-chain low molecular weight (LMW) FAs (e.g. Otto and Simpson, 2007), hopanoids (e.g. Gallegos, 1975; Mycke et al., 1987; Hofmann et al., 1992; Poerschmann et al., 2007; Berwick et al., 2010), and both branched (br-) and isoprenoid (i-) GDGTs (Simoneit, 1973; van den Berg et al., 1977; Michaelis and Albrecht, 1979; Kuypers et al., 2002; Pancost et al., 2008; Huguet et al., 2010a,b; Weijers et al., 2011), are part of kerogen and other forms of IOM. The observations in Chaves Torres and Pancost (2016) confirm that a variety of prokaryotic membrane lipids are part of the IOM of a *Sphagnum* peat bog. Moreover, those analyses suggested that the intact polar (IP) head groups of membrane lipids and the functional groups of other lipids likely play an important role in their insolubilization.

Based on those findings, the current study extends that approach to marine sediments in order to further understand why certain prokaryotic lipids are either inherently insoluble or become so during early diagenesis, providing insights into the nature of OM insolubilization in diverse environments. The methodology used is similar to the one described previously (Chaves Torres and Pancost, 2016), and it is mainly based on the comparison of solvent-extractable prokaryotic biomarkers with the non-extractable or insoluble counterparts after different hydrolysis steps. However, in the current investigation, OM associated with the removal of carbonates is also assessed. The target prokaryotic membrane biomarkers are *iso*- and *anteiso*- C_{15} and C_{17} FAs (branched FAs), geohopanoids such as bishomohopanoic acid and bishomohopanol, archaeol and both br- and i-GDGTs (see Appendix for structures). Such lipids, as opposed to others that derive from a variety of soluble and insoluble sources, are diagnostic for prokaryotic cells, facilitating their identification and source assignment in OM pools and, hence, the assessment of IOM formation. The use of other, less diagnostic biomarkers (e.g. unbranched FAs) could lead to misinterpretation, since they have multiple bacterial and eukaryotic sources and occur as both soluble lipids and as constituents of selectively preserved biomacromolecules, e.g. cutin (Tegelaar et al., 1989a) or suberin (Kolattukudy, 1980). These compounds are not representative of the great diversity of components in sedimentary OM and furthermore, we work on a limited number of samples, consequently, we caution against over-extrapolation of these empirical results. However, we propose that mechanistic insights or hypotheses derived from this work provide a platform for further investigation.

2. Methods

2.1. Samples

Marine sediments were collected from the Eastern South Atlantic Ocean (ESAO) during the UK-GEOTRACES cruise, GA10E on board the research vessel Discovery (D357). A detailed description of the setting has been previously published (Hardman-Mountford et al., 2003; Hernandez-Sanchez et al., 2014a,b and Refs. therein). Briefly, samples were collected from the continental slope offshore Cape Town (South Africa), a region influenced by the Agulhas current (Lutjeharms and Vanballegooyen, 1988; Lutjeharms, 2006) and also by the Cape Jet, a current flowing northwards around the Cape Peninsula (Shelton and Hutchings, 1982).

Two of the sediment cores that were collected have been analysed here (Table 1): from Station 0 (St0; 34.1S 17.5E; 246 m depth) and from Station 0.75 (St0.75; 34.3S 17.3E; 1182 m depth); they were collected using a box Connelly Mega corer device (10 cm length) and a box corer device (20 cm length), respectively. Based on measurements of excess ^{230}Th (^{230}Thxs; vertical flux) combined with dry bulk density (DBD), the age of the surface sediments of the stations (0-2 cm depth) is estimated to be less than 1000 y (Hernandez-Sanchez, M. T., pers. comm.). St0 is a dark fine-grained mixture of silt and clay, whereas St0.75 is a grey mixture of slightly thicker grains (sand, silt and clay), but both cores also contained carbonates most likely from a biogenic origin. Crucially, the St0.75 total organic carbon (TOC) content is higher than at St0 by a factor from ca. 2 to 5 (Table 1), reflecting deposition under a more productive regime and leading to more rapid consumption of O_2 in shallow sediments (Hernandez-Sanchez et al., 2014a). Prior to analysis, marine sediments were sliced into 2 cm depth intervals and stored at -20 °C. Once on land, samples were freeze-dried and stored again at -20 °C until analysis.

2.2. Experimental Procedure

Freeze-dried marine sediments were ground and homogenised, prior to sequential solvent-extractions and chemical degradation of the post-extraction residue (Fig. 1).

2.2.1. Solvent-extractions

The detailed experimental procedure for solvent-extractions has already been published (Chaves Torres and Pancost, 2016). Briefly, freeze-dried sediment sections (Table 1) were subjected to a Bligh and Dyer extraction (BD) (3x) with a mixture of buffered water (solution of 0.05M KH_2PO_4 in water, adjusted to pH 7.2 with NaOH pellets), $CHCl_3$ and MeOH (4:5:10, *v/v*). The extract E1BD (Fig. 1) was obtained and subsequently, the air-dried residue, R1BD, was extracted with Soxhlet 48 h (Sox) – reflux of DCM/MeOH (2:1, *v/v*) – to make sure we exhausted soluble-OM from the matrix. Free sulfur was removed from both extracts – E1BD and E2Sox – prior to instrument analysis by adding copper turnings that had been previously activated by 1M HCl_{aq}, rinsed with bi-distilled water (approx. 10x) and then cleaned with MeOH and DCM. Both E1BD and E2Sox were then kept for analysis.

2.2.2. Chemical degradation

The post-extraction residue R2Sox was air-dried and subjected to base hydrolysis (BHy; methods previously described in Chaves Torres and Pancost, 2016) to obtain extract E3BHy – this step aimed to cleave ester-bound moieties from the insoluble matrix. The post base-hydrolysed residue R3BHy was air-dried and then subjected to carbonate removal with HCl/MeOH and alternatively with HCl_{aq} (Fig. 1). This was performed by adding approx. 15 ml of 2N HCl 86 % in MeOH to ca. 10 g of R3BHy. Samples were then left 24h. Samples were centrifuged and the supernatant transferred to a separation funnel, and the residue was subsequently washed with H_2O, H_2O/MeOH and DCM. The combined supernatants were liquid-liquid extracted with DCM (3x), yielding E4-HCl/MeOH. Alternatively, carbonate was removed from a different portion of R3BHy, using 6M HCl_{aq} and the same methods as

described above to obtain E4-HCl_{aq}. The use of aqueous HCl aimed to enhance carbonate salts solubility and hence, removal from the IOM.

Acid methanolysis (AMe; for methods see Chaves Torres and Pancost, 2016) was performed only upon the post carbonate-removal residue R4-HCl/MeOH to obtain E5AMe. This step aimed to cleave amide-, glycosidic- and remaining ester-bound moieties from the IOM. Compounds released after chemical degradation and, therefore, occuring in E3BHy, E4-HCl_{aq}, E4-HCl/MeOH and E5AMe extracts are considered as non-extractable or insoluble as opposed to the ones obtained after strictly solvent-based extractions (E1BD and E2Sox). All extracts (Fig. 1) were subjected to GC-MS analysis to assess the distribution of *iso*- and *anteiso*- C_{15} and C_{17} FAs, bishomohopanoic acid, bishomohopanol and archaeol. Furthermore, all extracts (Fig. 1) were subjected to HPLC-MS to assess the distribution of br- and i-GDGTs. Details of the instrumental analysis have been recently published (Chaves Torres and Pancost, 2016), but GDGT distributions from the HCl_{aq} and HCl/MeOH fractions were determined using an updated method (Hopmans et al., 2016). The difference between these two methods is very small with an average deviation of 0.005 TEX_{86} units within a global subset of samples (Hopmans et al., 2016). Note that GDGT concentrations are only semi-quantitative, based on comparison to a C_{46} GDGT internal standard (Huguet et al., 2006; see Appendix); therefore, they can only be compared among other samples in this study. Relative abundances of GDGTs are determined assuming similar response factors.

2.3. Calculation of GDGT-based proxies

The comparison of soluble versus insoluble GDGT distributions is also assessed by examining variations in GDGT-based proxies among the different OM fractions, as well as mass-weighted combinations of extractable and IOM pools (Section 3.4). Aside from

providing further insight into extractable vs IOM partitioning, this analysis assesses the effect of insoluble GDGTs on the fidelity of widely used proxies.

The Branched and Isoprenoid Tetraether index (BIT) is typically used as tracer for terrestrial (soil bacterial) OC in sediments (Hopmans et al., 2004). Here, BIT values have been calculated including and excluding insoluble br-GDGTs and crenarchaeol, i.e. using the summed concentration of solvent-extracted and insoluble tetraethers or just the solvent-extracted analogues (Eq. 1; Section 3.4; see Appendix for compound structures). Based on daily measurements of an in–house generated marine standard, the long-term standard error of BIT is 0.0048.

$$\mathrm{BIT} = \frac{[\text{GDGT-I}] + [\text{GDGT-II}] + [\text{GDGT-III}]}{[\text{GDGT-I}] + [\text{GDGT-II}] + [\text{GDGT-III}] + [\text{Cren}]} \qquad \textit{Equation 1}$$

We have also calculated the the TetraEther indeX of tetraethers with 86 carbon atoms (TEX_{86}) as well as associated GDGT indices. TEX_{86} was first defined by Schouten et al., (2002) (Eq. 2), and is based on the i-GDGTs biosynthesized by marine Thaumarchaeota. In marine sediments, TEX_{86} correlates with mean annual sea surface temperatures (SST) in overlying waters. A re-evaluation of this relationship by Kim et al. (2010) yielded two indices for (1) the entire dataset (GDGT index-1; TEX_{86}^{L}; Eq. 3) and (2) for a subset of the dataset that excluded GDGT distributions from high-latitude settings (GDGT index-2; TEX_{86}^{H}; Eq. 4) (see Appendix for compound structures). Based on daily measurements of an in–house generated marine standard, the long-term the standard error the proxies is 0.0027 (TEX_{86}), 0.0020 (GDGT index-1) and 0.0019 (GDGT index-2).

$$TEX_{86} = \frac{[\text{GDGT-2}] + [\text{GDGT-3}] + [\text{Cren'}]}{[\text{GDGT-1}] + [\text{GDGT-2}] + [\text{GDGT-3}] + [\text{Cren'}]} \qquad \textit{Equation 2}$$

$$(TEX_{86}^{L})\ \text{GDGT index-1} = \log\left(\frac{[\text{GDGT-2}]}{[\text{GDGT-1}] + [\text{GDGT-2}] + [\text{GDGT-3}]}\right) \quad \textit{Equation 3}$$

(TEX_{86}^{H}) GDGT index-2

$$= \log\left(\frac{[\text{GDGT-2}] + [\text{GDGT-3}] + [\text{Cren'}]}{[\text{GDGT-1}] + [\text{GDGT-2}] + [\text{GDGT-3}] + [\text{Cren'}]}\right) \quad \textit{Equation 4}$$

3. Results

The extractable OM of continental shelf sediments offshore Cape Town is dominated by sterols, long chain alkenones and LMW and high molecular weight (HMW) alkanoic acids and alcohols. *n*-Alkanes are also observed in the marine sediments and they occur in both extractable and insoluble fractions, as observed in previous work (Amblès et al., 1996). A thorough analysis of biomarkers of these sediments is described elsewhere (Hernandez-Sanchez et al., 2014b). Here, we focus on prokaryotic membrane biomarkers, although other biomarker groups such as *n*-alkanes are invoked to facilitate interpretation.

3.1. Branched FAs

In the ESAO shallow marine sediments, the highest concentrations of total recovered branched FAs, i.e. the summed concentrations of solvent-extracted and insoluble branched FAs, occur at the surface at St0.75 (0.4 mg/g TOC); overall, concentrations decrease by about an order of magnitude through the upper 10 cm (Fig. 2c). Branched FAs in St0 sediments have similar but slightly lower concentrations (0.1 mg/g TOC), but concentrations increase with depth in the upper 10 cm (Fig. 2a).

In contrast, the proportions of non-extractable branched FAs – at both stations – are higher in the deepest sections of the core compared to the shallower ones, reaching up to 70 % in St0 and up to 50% in St0.75 (Figs. 2a and c). In both cases, the major proportion of insoluble branched FAs occurs in the BHy extracts, but they also occur in the AMe extracts

(up to 25 %). After dissolving carbonates with 2N HCl 86% in MeOH, a small amount of branched FAs was released (up to 10 % of the total FA pool) (Fig. 2a and c); however, when this dissolution was performed with 2N HCl_{aq}, the percentage of branched FAs released was up to 40 % of the total FA pool (Fig. 2b and d).

Ratios of branched FAs vs straight-chain FAs were calculated in order to assess the preferential occurrence of bacterial lipids in the IOM. In general, the ratio of branched versus straight-chain FAs, do not vary when comparing shallow vs deep sediments (Fig. 3), except for the combined soluble extracts at St0.75 (Fig. 3d), where the ratio decreases with depth by a factor of 2, and the AMe extracts at St0, where the ratio decreases by a factor of 4. When these ratios are compared among soluble, BHy and both HCl_{aq} and HCl/MeOH pools, branched vs. straight-chain FAs ratios markedly differ: with values of ca.1.1- 3.7 in combined soluble extracts, ca. 0.8-1.5 in extracts obtained after acidification and carbonate dissolution, and ca. 2.0-2.2 in BHy extracts. The range of AMe extracts ratios is similar to the one observed in combined soluble fractions (0.9 to 3.5).

3.2. Hopanoids

Most of the total recovered geohopanoids – combined bishomohopanoic acid and bishomohopanol – identified using these procedures (43- 97%) occurred in the BD extracts (Fig. 4), with St0 having overall higher total concentrations (ca. 0.3 mg/g TOC) than St0.75, except for the deepest layer at St0. At both stations the concentrations of hopanoids are lowest in the deepest section analysed. Similar to branched FAs, concentrations in the Sox extracts are low, typically representing less than 4% of the total hopanoids recovered with the current methodology. However, in St0.75 this percentage increases up to 20%. The non-extractable fraction is much smaller – generally less than 20% – but it increases up to 60% in St0 deeper sections and in St0.75-1 (Fig. 4d). When no HCl_{aq} treatment is performed upon

R2Sox (Fig. 4a and c), insoluble geohopanoids mostly occur in BHy extracts, which represents (66-100%) of the total non-extractable fraction. However, when carbonates are dissolved with HCl_{aq} up to 0.2 mg/g TOC of geohopanoids are obtained in E4-HCl_{aq}, representing in most sediment sections the major insoluble fraction (Fig. 4b and d).

3.3. Archaeol and GDGTs

Archaeol only occurs in the extractable fractions (see Supplementary Material), similar to what was observed in peat (Chaves Torres and Pancost, 2016). Moreover, all of the extractable archaeol occurs in the BD extracts. Concentrations of archaeol at both stations are ca. 30 µg/g TOC, and they are one order of magnitude lower in the deepest sections of the core.

GDGTs occur in both the extractable and non-extractable fractions (Fig. 5). Most of the extractable GDGTs occur in the BD fraction, with three exceptions: St0-1 (Fig. 5c and d) and St0.75-3 (Fig. 5g and h), where the major proportion of i-GDGTs occur in the BHy fraction; and St0.75-3, where the largest proportion of br-GDGTs occurs in the Sox and HCl/MeOH (Fig. 5e) or HCl_{aq} (Fig. 5f) fractions. The most abundant br-GDGTs in St0 are GDGT-II, IIb and III (Fig. 6a); similarly, GDGT-IIb and GDGT-III are generally the most abundant br-GDGTs in St0.75 (Fig. 6c). Total concentrations of br-GDGTs, i.e. summed concentrations of soluble and insoluble br-GDGTs, vary both down-core and between stations (Fig. 5a, b, e and f). Concentrations exhibit no down-core trend at St0 (2.0-14 µg/g TOC), whereas, at St0.75 (0.27-7.6 µg/g TOC), concentrations decrease down-core by about one order of magnitude. Furthermore, the proportions of insoluble br-GDGTs (of total br-GDGTs) also vary between the two stations, especially with respect to their down-core behaviour. At St0, the proportion of insoluble br-GDGTs is ca. 50% smaller that the deepest section of the core as compared to shallow sediments (Fig. 5a and b); on the contrary, at

St0.75, the proportion of insoluble br-GDGTs increases by a factor of 3 at the deepest section (Fig. 5e and f). In most cases the BHy fraction dominates the non-extractable component, with the combined proportion in the other IOM extracts – HCl/MeOH, AMe and HCl_{aq} – only ranging from 1 to 15 %, with the exception of St0.75-3 (up to 40%, Fig. 5e and f). Differences in the distribution of br-GDGTs in extractable versus non-extractable fractions are complex, with some br-GDGTs only occurring in the extractable fractions (Fig. 6). However, GDGT-IIb is generally more abundant than GDGT-III in the BHy and AMe extracts compared to the extractable counterparts (see also Supplementary Table).

Total concentrations of i-GDGTs exhibit almost identical behaviour to br-GDGTs (Fig. 5c, d, g and h), with no down-core trend in St0 and decreasing concentrations of i-GDGTs – up to one order of magnitude – in St0.75. The most abundant i-GDGTs are GDGT-0 and crenarchaeol at both stations (Fig. 6b and d). Interestingly, the ratio of insoluble versus soluble i-GDGTs is higher (up to 5 times) than the same ratio for br-GDGTs (Fig. 7) in all six samples.

3.4. GDGT-based proxies

BIT values have been calculated for every OM fraction (see Figure 1) and furthermore, for the combined soluble and insoluble fractions (Table 2). With the exception of St0.75-2, the BIT values of the total extractable (TE) pool (0.06-0.09) and the total recovered (TR) pool (0.03-0.07) are higher at St0 than St0.75. In both stations, however, total insoluble (TI) BIT values are always lower (by a factor of 1.3 to 11) than the TE-BIT analogue. Consequently, when both soluble and insoluble GDGTs are used to calculate TR-BIT, values are lower – by a factor of 1.2 to 1.8 – as compared to the TE-BIT values, with TE vs TR-BIT variations larger than the measurement error (Section 2.3).

TE-TEX_{86} values (Schouten et al., 2002) (Table 2) range from 0.32 to 0.53, with St0 having the lower values and hence, the lowest calculated SST (3 – 8 ºC, compared to 10 – 16 ºC St0.75). This relatively large variation, occurring amongst samples of different depth, appears to be restricted to extractable OM pools, because the corresponding TI-derived ratios are relatively stable (0.34-0.43) amongst all six sediments. Despite this variability, the overall differences in GDGT distribution between the TE, TI and TR fractions are small, as manifested in similar proxy values, i.e. variations less than 0.15 between TE- and TI-TEX_{86} indices. Consequently, the overall reconstructed SST estimates only differ between TE and TI pools by 0.3 to 5.2 ºC. These variations are larger than the measurement error (Section 2.3). However, all but the most extreme TE vs TI variations are within the standard error of the SST calibration (± 4ºC, Table 2).

4. Discussion

4.1. Biomarker derived insights into mechanisms of IOM formation in continental shelf sediments offshore Cape Town

The IOM in continental shelf sediments offshore Cape Town contains a significant proportion of the total prokaryotic lipid pool, including 20-70% of the branched FAs (Fig. 2), 5-60% of the geohopanoids (Fig. 4) and 2-70% of the GDGTs (Fig. 5). IOM proportions vary among compound types, sampling sites and core depth (Figs. 2, 4 and 5). We propose several complementary mechanisms that account for our observations (Section 3) and could provide new insights into OM insolubilization processes. First, association with authigenic carbonates, where precipitation of authigenic carbonates and incorporation of OM could afford progressive protection from solvent extraction (after e.g. Peckmann et al., 1999; Thiel et al., 2001; Ge et al., 2015; Mason et al., 2015). The large proportions of prokaryotic membrane lipids released by dissolution of carbonates with HCl_{aq} (Figs. 2, 4 and 5) – up to

50 % of the total recovered lipids in some cases – is most likely direct evidence for this mechanism. However, caution must be taken when interpreting this, because the process of sediment freeze-drying can occlude certain compounds to their matrices (e.g. McClymont et al., 2007). In this study, we propose that the lipid-carbonate natural association could be either sorptive or simple physical encapsulation in authigenic carbonate, but the release of *n*-alkanes, which lack functional moieities, by HCl_{aq} treatment suggests the latter. However, hydrolysis could also occur at room temperature under such acidic conditions (Ogliaruso and Wolfe, 1995), providing an alternative mechanism for the release of lipids. Further analysis is required to explore the potential physical-chemical association of microbially-derived OM to marine carbonates, but also to assess the potential OM trapped in clay minerals, either naturally or as a consequence of sample processing.

Second, esterification as a cross-linking reaction, which likely occur between intact prokaryotic lipids or degraded functionalised counterparts and reactive sites within the IOM. Particularly, we suggest that branched FAs and both br- and i-GDGTs (St0.75) can esterify with IOM during diagenesis, with evidence for this being the higher BHy proportions of such lipids in the deepest sections of the core (Figs. 2 and 5). Such a process would be analogous to the degradation-recondensation pathway proposed by Tissot and Welte (1984), i.e. random degradation and polymerization reactions of functionalised molecules during diagenesis yielding a more recalcitrant geomacromolecule, and this has been invoked to favour the insolubilization of even labile molecules such as peptides (Hsu and Hatcher, 2005). Moreover, this cross-linking can be analogous to the *in situ* specific polymerisation pathways proposed by previous investigations. For instance, Gupta et al. (2007a,c) provided evidence of the *in situ* polymerisation of labile compounds from plant leaves; moreover, specific cross-linking facilitated by free sulfur species (Sinninghe Damsté and de Leeuw, 1990; van Dongen et al., 2006) or oxidizing agents (Harvey et al., 1983; Versteegh et al., 2004) has been

proposed as a means of geomacromolecule formation. Here, in Cape Town sediments the proportions of branched FAs and GDGTs (St0.75) released after BHy are higher at the deepest sections of the core, suggesting that they might be incorporated into the IOM via esterification reactions, as inferred in previous studies (e.g. Naafs and van Bergen, 2002; Otto and Simpson, 2007; Weijers et al., 2011).

Furthermore, we propose that the above mentioned cross-linking reactions could also occur via IP head groups (e.g. Sturt et al., 2004), potentially explaining the different behaviour of different ether lipid classes. In our investigation of peat (Chaves Torres and Pancost, 2016), we observed that archaeol was associated solely with the soluble OM pool, whereas GDGTs were split between the two pools; moreover, the proportion of archaeal i-GDGTs in the IOM pool was greater than that of the bacterial br-GDGTs – consistent with previous work (e.g. Tierney et al., 2011; Weijers et al.,2011). We observe both of these features in these marine sediments and propose a variety of possible mechanisms that could contribute to this observation. One, this partitioning could arise from differences in the IP moieties in the source organisms. i-GDGTs commonly occur as glycolipids (e.g. Schouten et al., 2008; Liu et al., 2011; Lengger et al., 2012), and polar head groups containing glyco-moieties are generally more associated with i-GDGTs than with br-GDGTs (e.g. Sturt et al., 2004; Lipp and Hinrichs, 2009; Peterse et al., 2011). Furthermore, archaeol is frequently detected as a phospholipid (e.g. Sturt et al., 2004; Rossel et al., 2008; Kellermann et al., 2016). Based on these IP differences and on the fact that we find i-GDGTs preferentially in IOM fractions we infer that lipids containing glycosidic head groups are preferentially incorporated into the IOM with time, whereas lipids containing phosphatidic head groups are more prone to be solvent-extracted. The mechanisms for this is unclear but could involve more rapid degradation of the latter, inhibiting their incorporation into IOM, however there is extensive debate on the relative stability of glycolipids vs phospholipids (e.g. Logemann et

al., 2011; Elling et al., 2017), which presents an important caveat to this interpretation. Two, as an alternative mechanism br-GDGTs are likely derived from a terrestrial source and likely to have lost their reactive IP head groups during transport, thereby becoming less prone to being incorporated into IOM than the pelagic i-GDGTs. This explanation would not apply to those *in situ* produced br-GDGTs (after e.g. Peterse et al., 2009; Zhu et al., 2011; Zell et al., 2014). Furthermore, although the loss of IP moieties during transport is plausible in this setting, it does not explain why the same behaviour occurs in peat (Chaves Torres and Pancost, 2016). Nor does it explain the difference in behaviour between archaeol and i-GDGTs. Three,a potential third mechanism is that i-GDGTs, either intact or as core lipids, are more likely to resist diagenetic changes due to evolutionary stress adaptation,i.e. the unique membranes and biochemical pathways of Archaea are known to ensure archaeal cells' survival under chronic energy stress, (Valentine, 2007). As a consequence, i-GDGTs might be more prone to cross-linking reactions over time (although again, this does not explain the difference in behaviour between archaeol and i-GDGTs). Overall, it remains unclear why different groups of ether lipids exhibit different partitioning between insoluble and soluble fractions, but similar behaviour has now been observed in different previous studies (Tierney et al., 2011; Weijers et al., 2011; Chaves Torres and Pancost, 2016); above, we have proposed some mechanisms that require further exploration.

Finally, the occurrence of prokaryotic membrane lipids in IOM fractions can be due to the protection afforded by the intact cell, which has been shown to be inherently insoluble to solvent extraction (after e.g. Sinninghe Damsté et al., 2014). This feature of prokaryotic cells could be considered analogous to that of traditional recalcitrant biomacromolecules invoked for the selective preservation pathway – e.g. algaenan (Derenne et al., 1992; 1994) or cutin (Tegelaar et al., 1989a) – and could even afford protection against degradation. In this case, lipids that occurred in IOM fractions were not released from a geomacromolecule but instead

from intact cells, as inferred in previous work (e.g. Philp and Calvin, 1976; Sinninghe Damsté et al., 2014). In peat (Chaves Torres and Pancost, 2016) large proportions (up to 50%) of insoluble bacterial and archaeal lipids occur in even the shallowest sediments (5 cm depth), suggesting that at least some of that insoluble character reflects the inherent recalcitrance of prokaryotic cells. If so, proportions of prokaryotic lipids in IOM might be expected to decrease as the cell degrades; that is not observed and down-core profiles are complex, but that could reflect the competing effects of 1) degradation of cells mobilising lipids from the IOM to soluble OM pools vs 2) enhanced degradation of soluble prokaryotic lipids compared to the insoluble counterparts (Hatcher et al., 1983). We note that if the protection afforded by this mechanism differs among organisms and cellular structures, that could also explain the differences in behaviour among ether lipids.

Caution must be taken when analysing trends down-core, since only three depths have been analysed for each marine station (Table 1) and furthermore, because previous studies report an analytical error of ca. 10% in solvent extractions (e.g. Lengger et al., 2012) and ca. 7% error in hydrolyses (e.g. Otto and Simpson, 2007). However, all marine sediments in the current study have been subjected to the same sequence of treatments (Section 2), which enables the comparison of results. The proportion of insoluble branched FAs that occur in E3BHy, E4-HCl/MeOH and E5AMe (Fig. 2a and c) or E3BHy and E4-HCl_{aq} (Fig. 2b and d) are always higher – up to 4 times – in the deepest sections of the core. This is also observed for geohopanoids (Fig. 4), with the exception of St0.75 after treatment with HCl_{aq} (Fig. 4d). This contrasts our previous investigation of peat (Chaves-Torres and Pancost, 2016) and suggests that these compounds are being progressively incorporated into the IOM pool. Proportions of IOM bacterial and archaeal GDGTs exhibit more complex behaviour, also increasing with depth at St0.75 (Fig. 5e-h), but not at a different sampling site, St0 (Fig. 5a-d). However, in both cases trends differ from those from peat profiles, where proportions of

GDGTs in IOM fractions decrease with depth below the water table (Huguet et al., 2010a; Chaves Torres and Pancost, 2016). Similar results to what had been observed in peats had been obtained for podzols (Huguet et al., 2010b) and marine sediments (Weijers et al., 2011), and it suggests a dynamic exchange between IOM and soluble OM pools. Therefore, both IOM formation and its subsequent reactivity appears to be contingent to the depositional setting, and we propose that the association of prokaryotic lipids in the IOM pool of these marine sediments is relatively more stable in comparison with previous studies. This inferred stability of prokaryotic lipids in the IOM pool is consistent with the lack of variation in i-GDGT distributions with depth (TEX_{86} and GDGT-indices). TEX_{86} values (Schouten et al., 2002) (Table 2) vary by 0.21 among all TE fractions in all samples. This could be due to changes in the GDGT-producing prokaryotic communities with sediment depth or diagenetic processes, both of which might alter proxy values slightly (e.g. Schouten et al., 2002; Weijers et al., 2006; Harrison et al., 2009; Lipp and Hinrichs, 2009; Weijers et al., 2011). However, this large variation does not occur in TI-proxy values (e.g. TEX_{86} values only vary up to 0.09 amongst all six sediments), suggesting a more stable IOM pool compared to the extractable analogue. Tentatively, these observations suggest a marine IOM pool more insulated from diagenetic processes than the extractable counterpart and highlights how IOM behaviour differs among depositional environments.

4.2. Potential hierarchy of prokaryotic compounds in IOM formation

Among the types of prokaryotic lipids analysed – branched FAs, geohopanoids and both bacterial and archaeal ether lipids – there is a preferential occurrence of some in IOM as compared to the extractable fraction; this fact could provide insight into the relative importance of OM insolubilization mechanisms. Branched vs. straight-chain FAs ratios are typically lower in IOM as compared to soluble OM pools (Fig. 3), indicating that branched FAs are not preferentially associated with IOM compared to the straight-chain analogues; this

is consistent with the latter deriving from a range of inherently insoluble sources, such as cutin. Intriguingly, branched vs. straight ratios are lower in extracts obtained after dissolution of carbonates (E4-HCl_{aq} and E4-HCl/MeOH). This observation might reflect a certain role of branched FAs producing bacteria in the formation of those carbonates, but further work would be needed to explore the underlying mechanism.

Archaeol only occurs in solvent-extractable fractions, as discussed above and consistent with previous findings in peat (Chaves Torres and Pancost, 2016). The reasons for this remain unclear but could be due to archaeol being more prone to losing its IP head groups, perhaps via the rapid degradation of these reactive components during early diagenesis (Section 4.1), or the cells of archaeol-producing archaea failing to afford structural protection from solvent extraction. In contrast, GDGTs do occur in the IOM suggesting that differences in IP head groups, transport, diagenesis or other factors could be an important control in regulating OM insolubilization. It is also possible that the different partitioning of archaeol and GDGTs among soluble and insoluble fractions is due to the core structure (diether vs tetraether), i.e. stronger non-covalent interactions of the longer tetraether chains within the cell. Further work would be needed to explore these mechanisms but the fact that the same observation occurs in peat (Chaves Torres and Pancost, 2016) and in the current marine sediments merit further study.

More detailed examination of GDGT distributions in soluble and IOM fractions reveals more complex controls on the formation of the latter. Both GDGT-0 and crenarchaeol are the most abundant i-GDGTs in both marine stations and in all OM pools (Fig. 6). However, GDGT-0 to crenarchaeol ratios are typically larger in the IOM pools (Fig. 6b and d). In fact, GDGT-0 to crenarchaeol ratios for the combined insoluble extracts are 8 to 30% higher than for the combined soluble analogues (see also Supplementary Table). This difference has already been reported (Weijers et al., 2011). We suggest, given our previous

discussion, that GDGT-0 IP moieties might be more reactive than those of crenarchaeol or that crenarchaeol has undergone greater diagenesis (which is expected if a greater proportion of GDGT-0 is biosynthesised in sediments; e.g. Schouten et al., 1998). Nonetheless, the underlying mechanisms require further testing, particularly since there is no current robust evidence of IP head groups being significantly different between GDGT-0 and crenarchaeol (e.g. Elling et al., 2015).

Despite these differences in the preferential occurrence of specific ether lipids in the IOM, and the fact that as much as 80% of the GDGTs occurred in IOM fractions, the overall effect of including insoluble i-GDGTs in TEX_{86} and other GDGT-index calculations is small and results in values within the standard error of the reconstructed SST (Table 2). In contrast, BIT indices are affected by consideration of both soluble and IOM fractions, with TI-BIT values being lower than TE-BIT (Table 2). As discussed above, this is due to a preferential occurrence of i-GDGTs over br-GDGTs in the IOM fractions (Fig. 7), which is consistent with previous investigations (Weijers et al., 2011; Chaves Torres et al., 2016). Alongside evidence that br-GDGTs can be produced *in situ* (e.g. Peterse et al., 2009; Zhu et al., 2011; Zell et al., 2014), this presents another caveat to simplistic interpretation of extractable sedimentary GDGTs as OM source indicators, especially when BIT values are very low. Moreover, we caution against comparison of absolute BIT values in ancient settings to those in recent sediments, because it will be unclear how partitioning of GDGTs among extractable and insoluble fractions could have changed during diagenesis.

5. Conclusion

Marine IOM pools appear to be more stable than peat IOM as inferred from higher proportions of insoluble FAs, hopanoids (St0) and GDGTs (St0.75) in the deepest sediment sections analysed; in any case, proportions of insoluble prokaryotic lipids do not clearly

decrease as observed in peat. In addition, the relatively small variations in TEX_{86} and GDGT-indices in insoluble, relative to soluble, fractions also suggest that the former is relatively stable. It is difficult to extrapolate from the narrow window of prokaryotic lipids to the behaviour of the entire IOM pool, but these observations suggest that IOM in these continental shelf marine sediments may be indeed less reactive than soluble OM and that the formation of IOM facilitates overall OM preservation. The mechanisms we propose for IOM formation in this setting are mainly incorporation of OM into authigenic carbonates, cross-linking of FAs with the IOM via esterification reactions and more complex covalent interactions of other functional groups in lipids, including the polar head groups of membrane lipids. It is also likely that there is an inherent insolubility of some prokaryotic lipids associated with cells, because the lipids are associated with IOM in the shallowest sediments. There is a bias in the partitioning of different compound classes (or even different compounds in the same class) among IOM pools. Archaeol occurs solely in soluble OM fractions, but up to 80 % of GDGTs occur in IOM fractions, with GDGT-0 more prone to be found in IOM fractions than crenarchaeol. There is also a clear preferential occurrence of archaeal GDGTs vs. bacterial GDGTs in the IOM pools. These latter observations are identical to those made for peat deposits, suggesting that similar processes may govern the formation of IOM, at least with respect to incorporation of prokaryotic lipids, in diverse settings.

Acknowledgements

This work was carried out thanks to the Eglinton Scholarship and we gratefully thank Professor Geoff Eglinton for his support and guidance. The authors would like to additionally thank the NERC for funding the UK-GEOTRACES programme (NE/F019076/1); and the officers, crew and technical support on RV Discovery cruise D357. We gratefully acknowledge Mrs. Alison Kuhl, Mr. James Williams, Dr. Ian Bull and the NERC LSMSF (Bristol node). We also acknowledge Mr. Des Davis from the Microanalytical Laboratory,

School of Chemistry (Bristol University). RDP acknowledges the RS Wolfson Research Merit Award and the ERC Grant T-GRES (Project Reference 340923).

CAPTIONS

Figure 1. Schematic flow chart of the experimental procedure applied on marine sediments.

Figure 2. Percentage relative abundances of branched FAs at St0 (top) and St0.75 (bottom) after BD, Sox, BHy HCl/MeOH and AMe (a and c) and BD, Sox, BHy and HCl_{aq} (b and d). Numbers within bars are concentrations of branched FAs (µg/g TOC).

Figure 3. Ratio of branched versus straight-chain FAs in combined extractable fractions (a and d), after dissolution of carbonates with HCl (b and e) and after base and acid hydrolysis (c and f), in St0 (top) and St0.75 (bottom).

Figure 4. Percentage relative abundances of total hopanoids (bishomohopanoic acids and bishomohopanol) in Station 0 (top) and Station 0.75 (bottom), after BD, Sox, BHy, HCl/MeOH and AMe (a and c); and BD, Sox, BHy and HCl_{aq} (b and d). Note that numbers within bars are concentrations of hopanoids expressed in µg/g TOC.

Figure 5. Percentage relative abundances of GDGTs from St0 (top; a-d) and St0.75 (bottom; e-h), after BD, Sox, BHy, HCl/MeOH and AMe or, alternatively, BD, Sox, BHy and HCl_{aq}. Numbers within bars are concentrations of GDGTs (µg/g TOC) obtained after semi-quantification using internal standard (Section 2.2.2).

Figure 6. Distribution of bacterial and archaeal GDGTs from St0 (a and b, respectively) and from St0.75 (c and d, respectively) after BD, Sox, BHy, HCl/MeOH, AMe and HCl_{aq}. See also ST for detailed concentrations.

Figure 7. Ratio of non-extractable or insoluble GDGTs (in fractions BHy, HCl/MeOH and AMe; or alternatively, BHy and HCl_{aq}) versus the extractable counterparts (in BD and Sox fractions).

Appendix

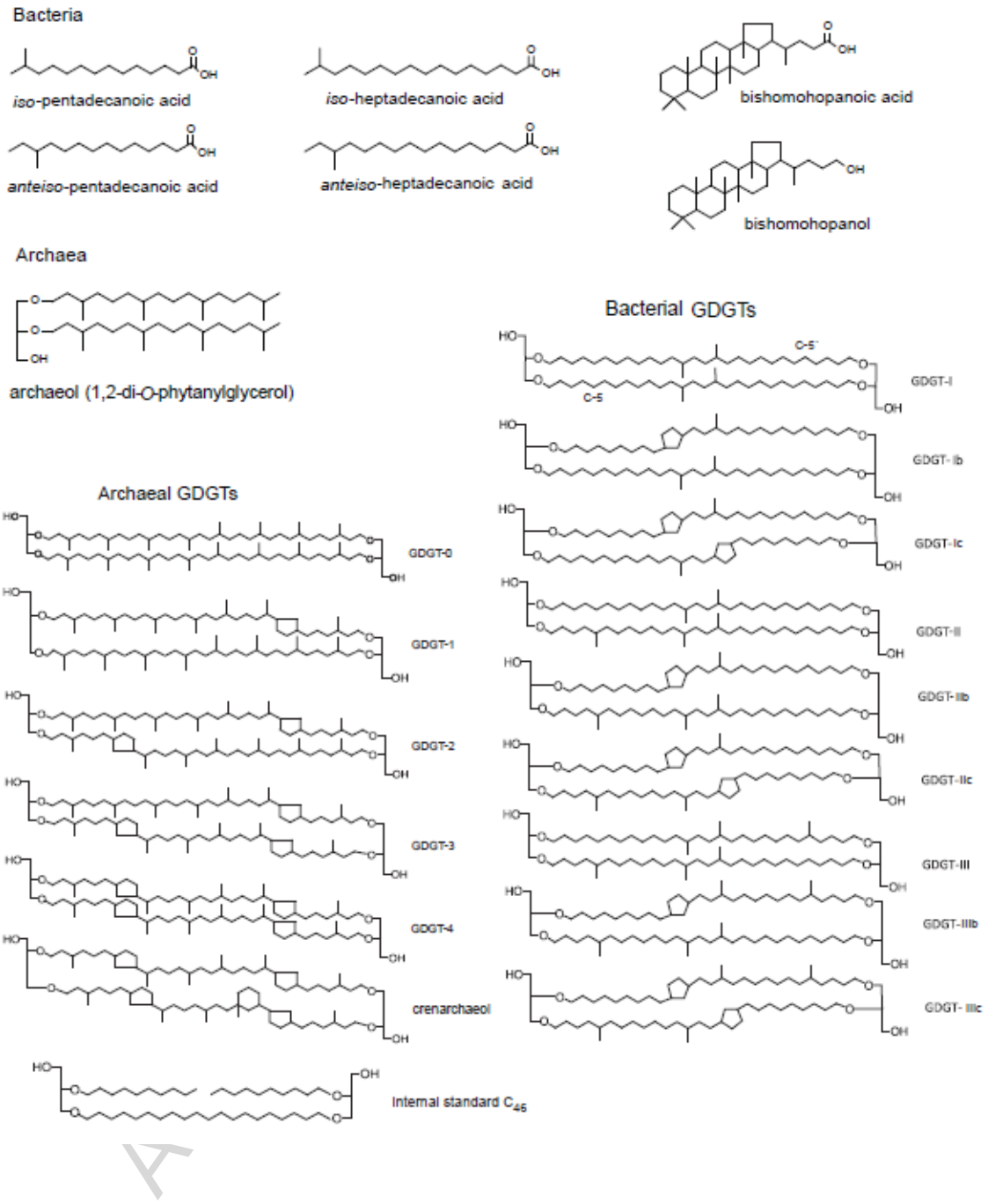

References

Amblès, A., Grasset, L., Dupas, G. and Jacquesy, J.-C., 1996. Ester- and ether bond cleavage in immature kerogens. Organic Geochemistry, 24(6-7): 681-690.

Berger, W.H., Smetacek, V.S. and Wefer, G., 1989. Ocean productivity and paleoproductivity: an overview. In: W.H. Berger, V.S. Smetacek and G. Wefer (Editors), Productivity of the Ocean: Present and Past. Wiley, pp. 1-34.

Berwick, L.J., Greenwood, P.F., Meredith, W., Snape, C.E. and Talbot, H.M., 2010. Comparison of microscale sealed vessel pyrolysis (MSSVpy) and hydropyrolysis (Hypy) for the characterisation of extant and sedimentary organic matter. Journal of Analytical and Applied Pyrolysis, 87(1): 108-116.

Chaves Torres, L. and Pancost, R.D., 2016. Insoluble prokaryotic membrane lipids in a *Sphagnum* peat: Implications for organic matter preservation. Organic Geochemistry, 93: 77-91.

de Leeuw, J.W., 2007. On the origin of sedimentary aliphatic macromolecules: A comment on recent publications by Gupta et al. Organic Geochemistry, 38: 1585-1587.

Derenne, S., Largeau, C. and Behar, F., 1994. Low polarity pyrolysis products of Permian to Recent Botryococcus-rich sediments: First evidence for the contribution of an isoprenoid algaenan to kerogen formation. Geochimica et Cosmochimica Acta, 58(17): 3703-3711.

Derenne, S., Largeau, C., Casadevall, E. and Connan, J., 1988. Comparison of torbanites of various origins and evolutionary stages. Bacterial contribution to their formation. Causes of the lack of botryococcane in bitumens. Organic Geochemistry, 12(1): 43-59.

Derenne, S., Largeau, C. and Hatcher, P.G., 1992. Structure of Chlorella fusca algaenan: relationships with ultralaminae in lacustrine kerogens; species- and environment-dependent variations in the composition of fossil ultralaminae. Organic Geochemistry, 18(4): 417-422.

Elling, F.J., Könneke, M., Mußmann, M., Greve, A., Hinrichs, K-U., 2015. Influence of temperature, pH, and salinity on membrane lipid composition and TEX_{86} of marine planktonic thaumarchaeal isolates. Geochimica et Cosmochimica Acta 171, 238-255.Elling, F.J., Könneke, M., Nicol, G.W., Stieglmeier, M., Bayer, B., Spieck, E., de la Torre, J.R., Becker, K.W., Thomm, M., Prosser, J.I., Herndl, G.J., Schleper, C, Hinrichs, K-U., 2017. Chemotaxonomic characterisation of the thaumarchaeal lipidome. Environmental Microbiology 19, 2681-2700.

Gallegos, E.J., 1975. Terpane-sterane release from kerogen by pyrolysis-gas chromatography mass spectrometry. Analytical Chemistry, 47(9): 1524-1528.

Garcette-Lepecq, A., Largeau, C., Bouloubassi, I., Derenne, S., Saliot, A., Lorre, A., Point, V., 2004. Lipids and their modes of occurrence in two surface sediments from the Danube delta and northwestern Black Sea: implications for sources and early diagenetic alteration: I. Carboxylic acids. Organic Geochemistry, 35(8): 959-980.

Ge, L., Jiang, S.Y., Blumenberg, M., Reitner, J., 2015. Lipid biomarkers and their specific carbon isotopic compositions of cold seep carbonates from the South China Sea. Marine and Petroleum Geology, 66: 501-510.

Gupta, N.S. et al., 2007. Evidence for the *in situ* polymerisation of labile aliphatic organic compounds during the preservation of fossil leaves: Implications for organic matter preservation. Organic Geochemistry, 38(3): 499-522.

Gupta, N.S. et al., 2007. De Leeuw comment "On the origin of sedimentary aliphatic macromolecules". Organic Geochemistry, 38(9): 1588-1591.

Gupta, N.S. et al., 2007. Experimental evidence for the formation of geomacromolecules from plant leaf lipids. Organic Geochemistry, 38(1): 28-36.

Hardman-Mountford, N.J. et al., 2003. Ocean climate of the South East Atlantic observed from satellite data and wind models. Progress in Oceanography, 59(2–3): 181-221.

Harrison, B.K., Zhang, H., Berelson, W. and Orphan, V.J., 2009. Variations in archaeal and bacterial diversity associated with the sulfate-methane transition zone in continental margin sediments (Santa Barbara Basin, California). Applied and Environmental Microbiology, 75(6): 1487-1499.

Harvey, G.R., Boran, D.A., Chesal, L.A. and Tokar, J.M., 1983. The structure of marine fulvic and humic acids. Marine Chemistry, 12(2-3): 119-132.

Harvey, H.R., 2006. Sources and cycling of organic matter in the marine water column. In: J. Volkman (Editor), The Handbook of Environmental Chemistry. Marine Organic Matter: Biomarkers, Isotopes and DNA, pp. 1-27.

Hatcher, P.G. et al., 1996. Encapsulation of microbiologically labile compounds within macromolecular organic matter in sedimentary systems as a means of preservation. Abstracts of Papers of the American Chemical Society, 212: 39-GEOC.

Hatcher, P.G., Spiker, E.C., Szeverenyi, N.M. and Maciel, G.E., 1983. Selective preservation and origin of petroleum-forming aquatic kerogen. Nature, 305(5934): 498-501.

Hernandez-Sanchez, M.T., Homoky, W.B. and Pancost, R.D., 2014a. Occurrence of 1-*O*-monoalkyl glycerol ether lipids in ocean waters and sediments. Organic Geochemistry, 66: 1-13.

Hernandez-Sanchez, M.T. et al., 2014b. Further insights into how sediment redox status controls the preservation and composition of sedimentary biomarkers. Organic Geochemistry, 76: 220-234.

Hofmann, I.C., Hutchison, J., Robson, J.N., Chicarelli, M.I. and Maxwell, J.R., 1992. Evidence for sulfide links in a crude-oil asphaltene and kerogens from reductive cleavage by lithium in ethylamine. Organic Geochemistry, 19(4-6): 371-387.

Hopmans, E.C., Schouten, S. and Sinninghe Damsté, J.S., 2016. The effect of improved chromatography on GDGT-based palaeoproxies. Organic Geochemistry, 93: 1-6.

Hopmans, E.C. et al., 2004. A novel proxy for terrestrial organic matter in sediments based on branched and isoprenoid tetraether lipids. Earth and Planetary Science Letters, 224(1-2): 107-116.

Hsu, P.H. and Hatcher, P.G., 2005. New evidence for covalent coupling of peptides to humic acids based on 2D NMR spectroscopy: A means for preservation. Geochimica Et Cosmochimica Acta, 69(18): 4521-4533.

Huguet, A., Fosse, C., Laggoun-Defarge, F., Toussaint, M.-L. and Derenne, S., 2010a. Occurrence and distribution of glycerol dialkyl glycerol tetraethers in a French peat bog. Organic Geochemistry, 41(6): 559-572.

Huguet, A., Fosse, C., Metzger, P., Fritsch, E. and Derenne, S., 2010b. Occurrence and distribution of non-extractable glycerol dialkyl glycerol tetraethers in temperate and tropical podzol profiles. Organic Geochemistry, 41(8): 833-844.

Huguet, C. et al., 2006. An improved method to determine the absolute abundance of glycerol dibiphytanyl glycerol tetraether lipids. Organic Geochemistry, 37(9): 1036-1041.

Kellermann, M.Y., Yoshinaga, M.Y., Wegener, G., Krukenberg, V. and Hinrichs, K.-U., 2016. Tracing the production and fate of individual archaeal intact polar lipids using stable isotope probing. Organic Geochemistry, 95: 13-20.

Kim, J.-H. et al., 2010. New indices and calibrations derived from the distribution of crenarchaeal isoprenoid tetraether lipids: Implications for past sea surface temperature reconstructions. Geochimica et Cosmochimica Acta, 74(16): 4639-4654.

Kolattukudy, P.E., 1980. Biopolyester Membranes of Plants: Cutin and Suberin. Science, 208(4447): 990-1000.

Kuypers, M.M.M. et al., 2002. Archaeal remains dominate marine organic matter from the early Albian oceanic anoxic event 1b. Palaeogeography Palaeoclimatology Palaeoecology, 185(1-2): 211-234.

Largeau, C., Casadevall, E., Kadouri, A. and Metzger, P., 1984. Formation of *Botryococcus braunii* Kerogens. Comparative study of immature Torbanite and of the extant alga *Botryococcus braunii*. Organic Geochemistry, 6: 327-332.

Largeau, C., Derenne, S., Casadevall, E., Kadouri, A. and Sellier, N., 1986. Pyrolysis of immature Torbanite and of the resistant biopolymer (PRB A) isolated from extant alga *Botryococcus braunii*. Mechanism of formation and structure of torbanite. Organic Geochemistry, 10(4-6): 1023-1032.

Lengger, S.K., Hopmans, E.C., Sinninghe Damsté, J.S. and Schouten, S., 2012. Comparison of extraction and work up techniques for analysis of core and intact polar tetraether lipids from sedimentary environments. Organic Geochemistry, 47: 34-40.

Lengger, S.K., Hopmans, E.C., Sinninghe Damsté, J.S. and Schouten, S., 2014. Fossilization and degradation of archaeal intact polar tetraether lipids in deeply buried marine sediments (Peru Margin). Geobiology, 12(3): 212-220.

Lipp, J.S. and Hinrichs, K.-U., 2009. Structural diversity and fate of intact polar lipids in marine sediments. Geochimica et Cosmochimica Acta, 73(22): 6816-6833.

Liu, X., Lipp, J.S. and Hinrichs, K.-U., 2011. Distribution of intact and core GDGTs in marine sediments. Organic Geochemistry, 42(4): 368-375.

Logemann, J., Graue, J., Köster, J., Engelen, B., Rullkötter, J., Cypionka, H., 2011. A laboratory experiment of intact polar lipid degradation in sandy sediments. Biogeosciences 8, 2547–2560.Lutjeharms, J.R.E., 2006. The Agulhas Current. Springer-Verlag, Germany.

Lutjeharms, J.R.E. and Van Ballegooyen, R.C., 1988. The retroflection of the Agulhas Current. Journal of Physical Oceanography, 18(11): 1570-1583.

Mason, O.U., Case, D.H., Naehr, T.H., Raymond, W.L., Thomas, R.B., Bailey, J.V., Orphan, V.J., 2015. Comparison of archaeal and bacerial diversity in methane seep carbonate nodules and host sediments, Eel river basin and Hydrate Ridge, USA. Microbial Ecology, 70(3): 766-784.

McClymont, E.L., Martínez-Garcia, A. and Rosell-Melé, A., 2007. Benefits of freeze-drying sediments for the analysis of total chlorins and alkenone concentrations in marine sediments. Organic Geochemistry, 38(6): 1002-1007.

Michaelis, W. and Albrecht, P., 1979. Molecular fossils of archaebacteria in kerogen. Naturwissenschaften, 66(8): 420-422.

Mycke, B., Narjes, F. and Michaelis, W., 1987. Bacteriohopanetetrol from chemical degradation of an oil-shale kerogen. Nature, 326(6109): 179-181.

Naafs, D.F.W. and van Bergen, P.F., 2002. A qualitative study on the chemical composition of ester-bound moieties in an acidic andosolic forest soil. Organic Geochemistry, 33(3): 189-199.

Ogliaruso, M.A., Wolfe, J.F., 1995. Carboxylic acids. In: A.R. Katritzky, Meth-Cohn, O., Rees, C.W. (Editor), Comprehensive Organic Functional Group Transformations. Elsevier Science, Oxford, UK, pp. 23-120.

Otto, A. and Simpson, M.J., 2007. Analysis of soil organic matter biomarkers by sequential chemical degradation and gas chromatography - mass spectrometry. Journal of Separation Science, 30(2): 272-282.

Pancost, R.D. et al., 2008. Kerogen-bound glycerol dialkyl tetraether lipids released by hydropyrolysis of marine sediments: A bias against incorporation of sedimentary organisms? Organic Geochemistry, 39(9): 1359-1371.

Peckmann, J., Thiel, V., Michaelis, W., Clari, P., Gaillard, C., Martire, L., Reitner, J., 1999. Cold seep deposits of Beauvoisin (Oxfordian; southeastern France) and Marmorito (Miocene; northern Italy): microbially induced authigenic carbonates. International Journal of Earth Sciences, 88(1): 60-75.

Peterse, F. et al., 2011. Identification and distribution of intact polar branched tetraether lipids in peat and soil. Organic Geochemistry, 42(9): 1007-1015.

Peterse, F. et al., 2009. Constraints on the application of the MBT/CBT palaeothermometer at high latitude environments (Svalbard, Norway). Organic Geochemistry, 40(6): 692-699.

Philp, R.P. and Calvin, M., 1976. Possible origin for insoluble organic (kerogen) debris in sediments from insoluble cell-wall materials of algae and bacteria. Nature, 262(5564): 134-136.

Poerschmann, J., Trommler, U., Fabbri, D. and Gorecki, T., 2007. Combined application of non-discriminated conventional pyrolysis and tetramethylammonium hydroxide-induced thermochemolysis for the characterization of the molecular structure of humic acid isolated from polluted sediments from the Ravenna Lagoon. Chemosphere, 70(2): 196-205.

Ronov, A.B., Yaroshevsky, A.A. and Migdisov, A.A., 1990. Chemical Structure of the Earth´s Crust and Chemical Balance of Major Elements. Izdatel´stvo, Moscow.

Rossel, P.E. et al., 2008. Intact polar lipids of anaerobic methanotrophic archaea and associated bacteria. Organic Geochemistry, 39(8): 992-999.

Rullkötter, J. and Michaelis, W., 1990. The structure of kerogen and related materials. A review of recent progress and future trends. Organic Geochemistry, 16(4-6): 829-852.

Schidlowski, M., 2001. Carbon isotopes as biogeochemical recorders of life over 3.8 Ga of Earth history: evolution of a concept. Precambrian Research, 106(1-2): 117-134.

Schouten, S. et al., 2008. Intact membrane lipids of "Candidatus Nitrosopumilus maritimus," a cultivated representative of the cosmopolitan mesophilic group I crenarchaeota. Applied and Environmental Microbiology, 74(8): 2433-2440.

Schouten, S., Hopmans, E.C. and Damste, J.S.S., 2013. The organic geochemistry of glycerol dialkyl glycerol tetraether lipids: A review. Organic Geochemistry, 54: 19-61.

Schouten, S., Hopmans, E.C., Schefuss, E. and Sinninghe Damsté, J.S., 2002. Distributional variations in marine crenarchaeotal membrane lipids: a new tool for reconstructing ancient sea water temperatures? Earth and Planetary Science Letters, 204(1-2): 265-274.

Schouten, S., Middelburg, J.J., Hopmans, E.C. and Sinninghe Damsté, J.S., 2010. Fossilization and degradation of intact polar lipids in deep subsurface sediments: A theoretical approach. Geochimica et Cosmochimica Acta, 74: 3806-3814.

Shelton, P.A., Hutchings, L., 1982. Transport of anchovy, *Engraulis capensis* Gilchrist, eggs and early larvae by a frontal jet current. Journal du Conseil, 40: 185-198.

Simoneit, B.R. and Burlingame, A.L., 1973. Carboxylic acids derived from Tasmanian tasmanite by extractions and kerogen oxidations. Geochimica et Cosmochimica Acta, 37(3): 595-610.

Sinninghe Damsté, J.S. and De Leeuw, J.W., 1990. Analysis, structure and geochemical significance of organically-bound sulphur in the geosphere: State of the art and future research. Organic Geochemistry, 16(4-6): 1077-1101.

Sinninghe Damsté, J.S. et al., 2014. Ether- and Ester-Bound iso-Diabolic Acid and Other Lipids in Members of Acidobacteria Subdivision 4. Applied and Environmental Microbiology, 80(17): 5207-5218.

Sturt, H.F., Summons, R.E., Smith, K., Elvert, M. and Hinrichs, K.U., 2004. Intact polar membrane lipids in prokaryotes and sediments deciphered by high-performance liquid chromatography/electrospray ionization multistage mass spectrometry - new biomarkers for biogeochemistry and microbial ecology. Rapid Communications in Mass Spectrometry, 18(6): 617-628.

Tegelaar, E.W. et al., 1989a. Scope and limitations of several pyrolysis methods in the structural elucidation of a macromolecular plant constituent in the leaf cuticle of *Agave americana* L. Journal of Analytical and Applied Pyrolysis, 15: 29-54.

Tegelaar, E.W., Deleeuw, J.W., Derenne, S. and Largeau, C., 1989b. A reppraisal of kerogen formation. Geochimica Et Cosmochimica Acta, 53(11): 3103-3106.

Thiel, V. et al., 2001. Molecular signals for anaerobic methane oxidation in Black Sea seep carbonates and a microbial mat. Marine Chemistry, 73(2): 97-112.

Tierney, J.E., Schouten, S., Pitcher, A., Hopmans, E.C., Sinninghe Damsté, J.S., 2011. Core and intact polar glycerol dialkyl glycerol tetraethers (GDGTs) in Sand Pond Warwick,, Rhode Island (USA): Insights into the origin of lacustrine GDGTs. Geochimica et cosmochimica Acta 77, 561-581.

Tissot, B.P. and Welte, D.H., 1984. Petroleum Formation and Occurrence. Springer.

Valentine, D.L., 2007. Adaptations to energy stress dictate the ecology and evolution of the Archaea. Nature Reviews Microbiology, 5(4): 316-323.

van Den Berg, M.L.J., Mulder, G.J., De Leeuw, J.W. and Schenck, P.A., 1977. Investigations into the structure of kerogen-I. Low temperature ozonolysis of Messel shale kerogen. Geochimica Et Cosmochimica Acta, 41(7): 903-908.

van Dongen, B.E., Schouten, S. and Damste, J.S.S., 2006. Preservation of carbohydrates through sulfurization in a Jurassic euxinic shelf sea: Examination of the Blackstone Band TOC cycle in the Kimmeridge Clay Formation, UK. Organic Geochemistry, 37(9): 1052-1073.

Vandenbroucke, M. and Largeau, C., 2007. Kerogen origin, evolution and structure. Organic Geochemistry, 38(5): 719-833.

Versteegh, G.J.M. et al., 2004. An example of oxidative polymerization of unsaturated fatty acids as a preservation pathway for dinoflagellate organic matter. Organic Geochemistry, 35(10): 1129-1139.

Weijers, J.W.H., Lim, K.L.H., Aquilina, A., Sininghe Damsté, J.S. and Pancost, R.D., 2011. Biogeochemical controls on glycerol dialkyl glycerol tetraether lipid distributions in sediments characterized by diffusive methane flux. Geochemistry Geophysics Geosystems, 12: 1-15.

Weijers, J.W.H., Schouten, S., Spaargaren, O.C. and Sinninghe Damsté, J.S., 2006. Occurrence and distribution of tetraether membrane lipids in soils: Implications for the use of the TEX_{86} proxy and the BIT index. Organic Geochemistry, 37(12): 1680-1693.

Zell, C. et al., 2014. Sources and distributions of branched and isoprenoid tetraether lipids on the Amazon shelf and fan: Implications for the use of GDGT-based proxies in marine sediments. Geochimica et Cosmochimica Acta, 139: 293-312.

Zhu, C., Talbot, H.M., Wagner, T., Pan, J.M. and Pancost, R.D., 2011. Distribution of hopanoids along a land to sea transect: Implications for microbial ecology and the use of hopanoids in environmental studies. Limnology and Oceanography, 56(5): 1850-1865.

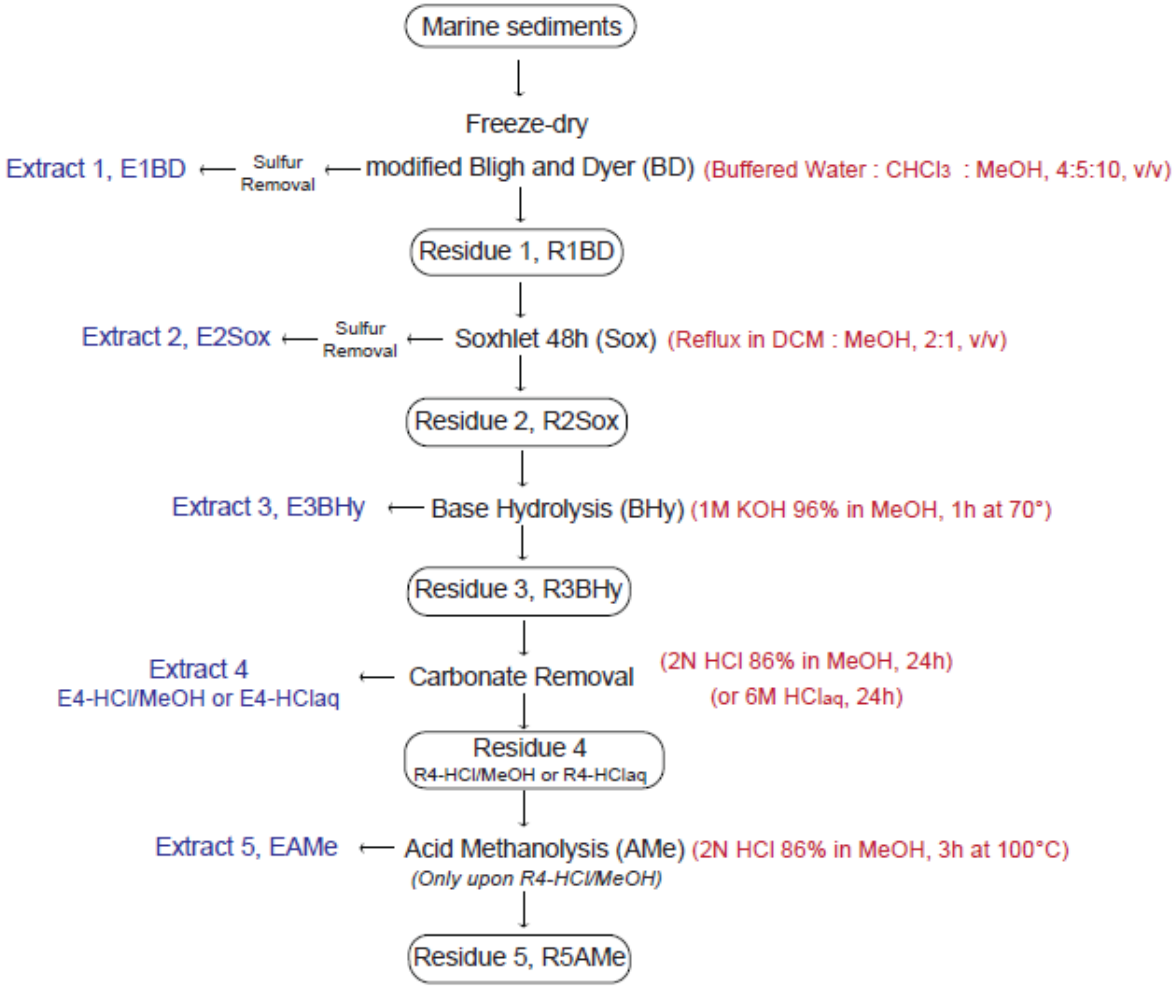

Fig. 1

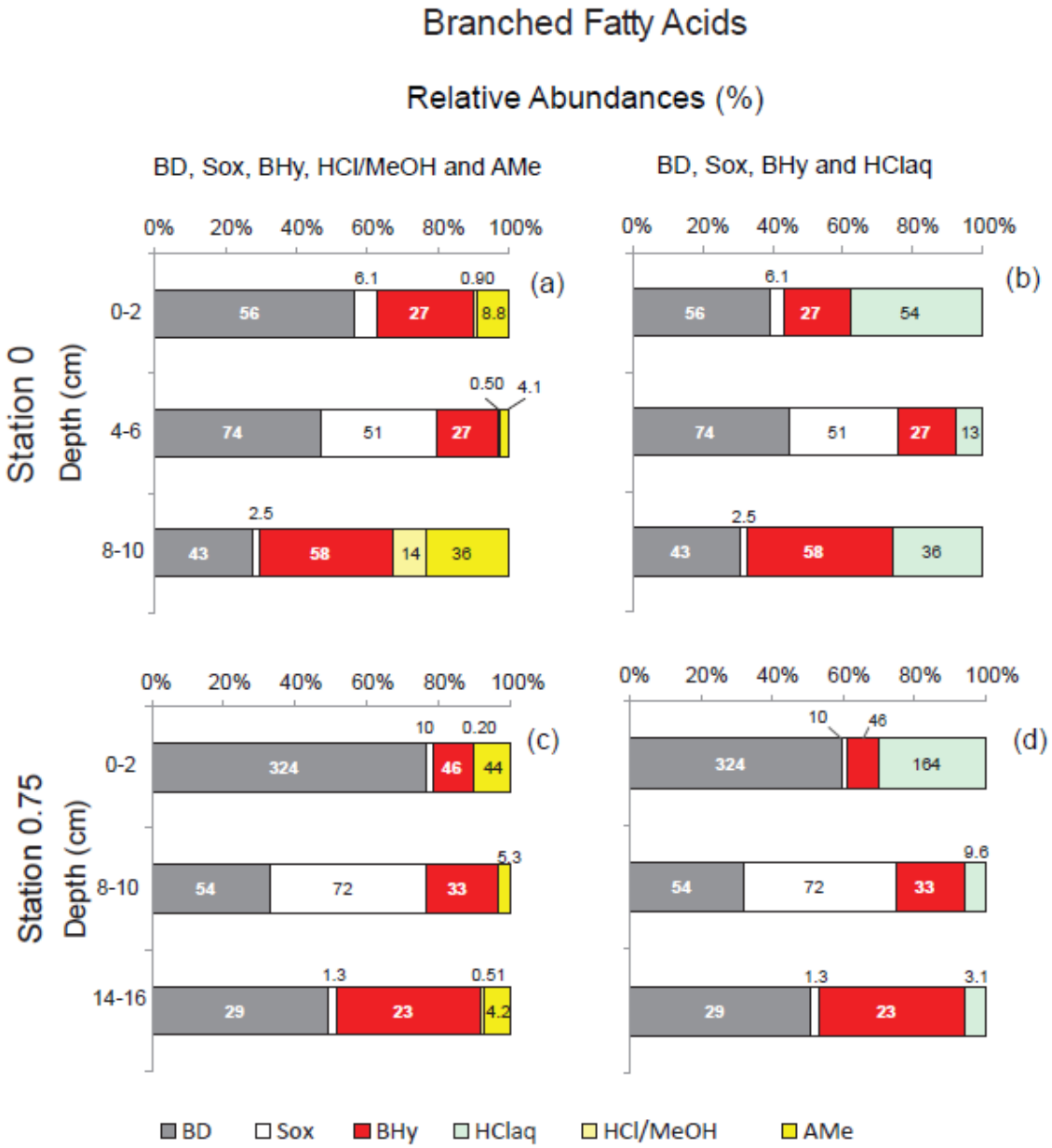

Fig. 2

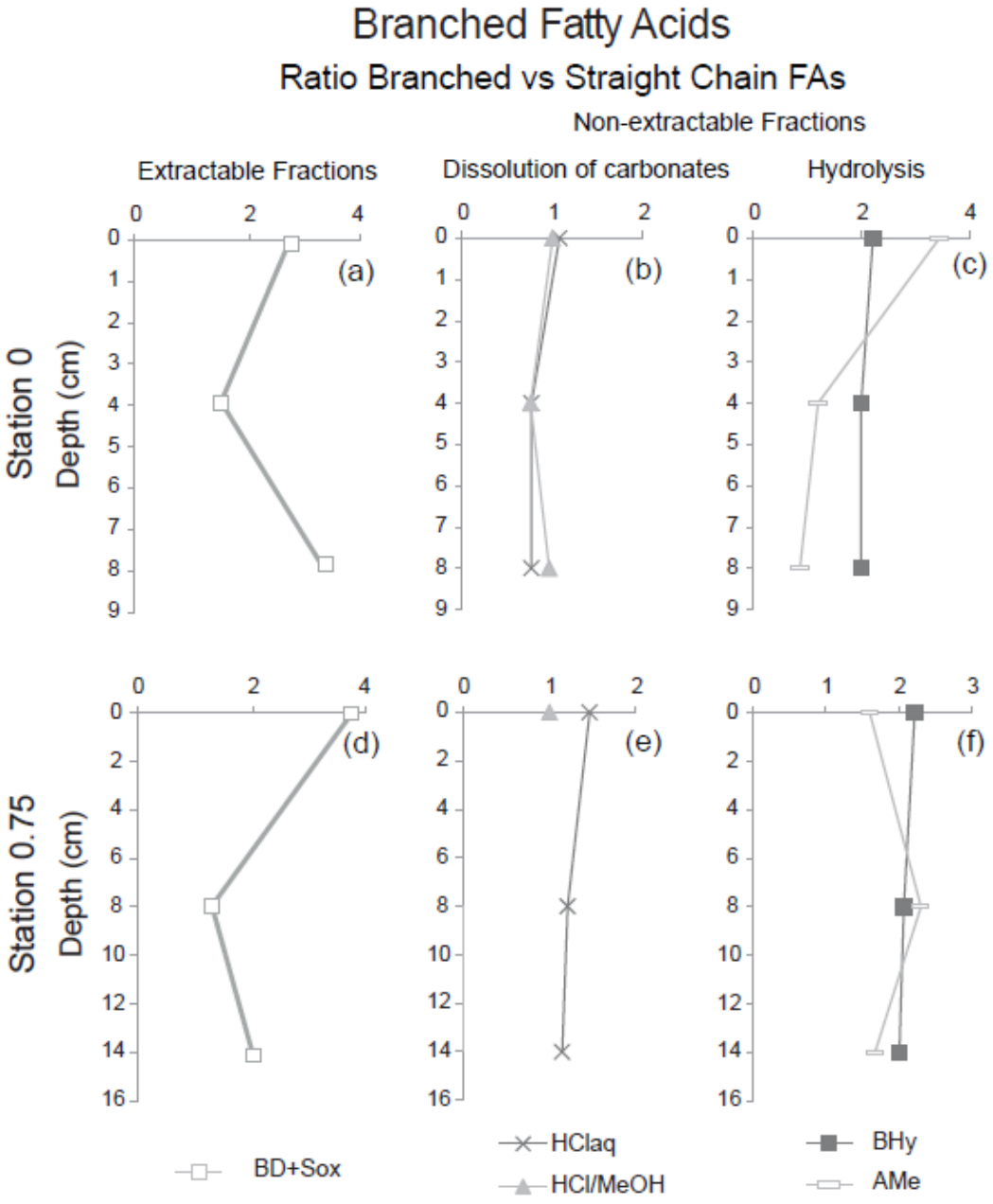

Fig. 3

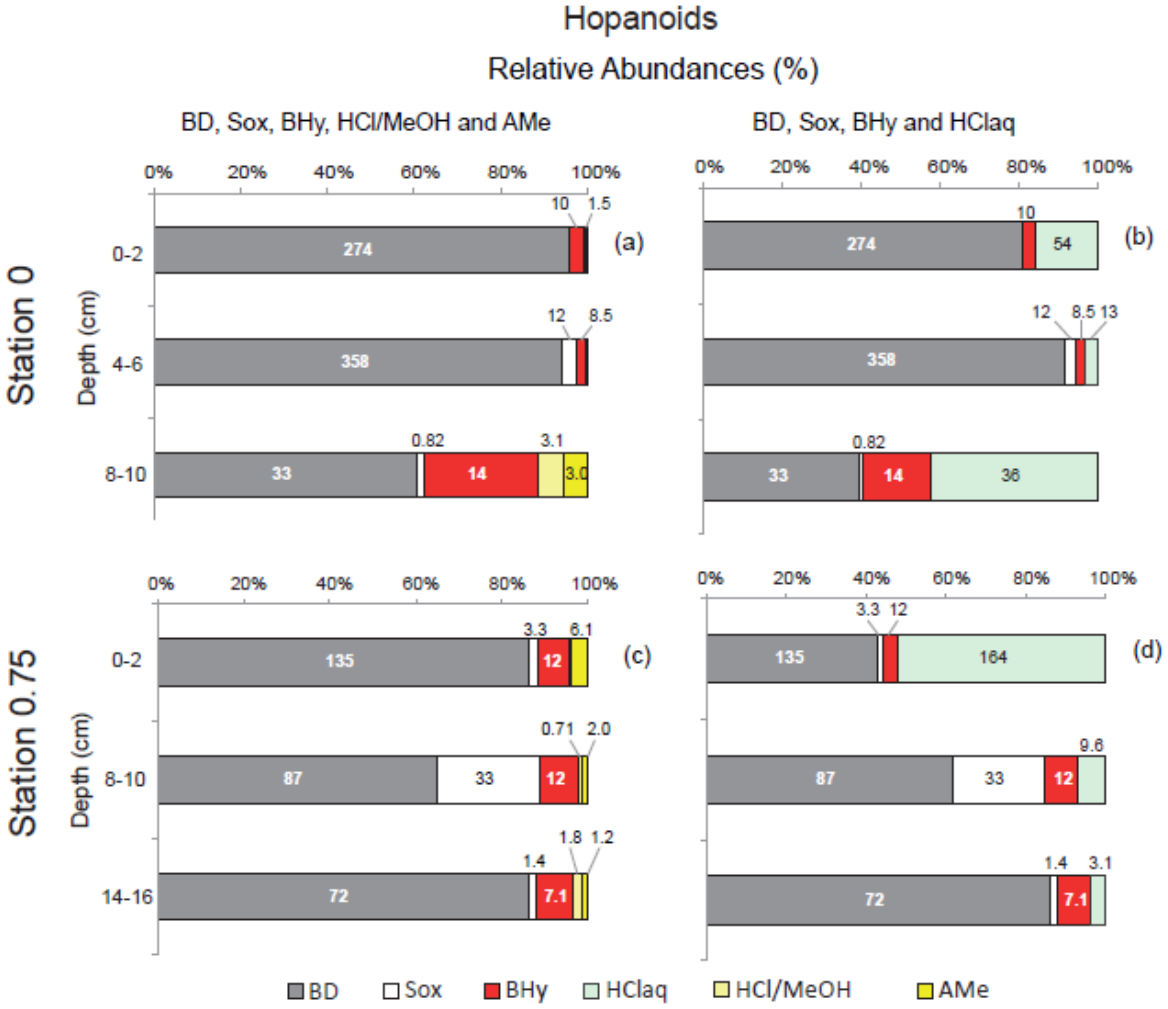

Fig. 4

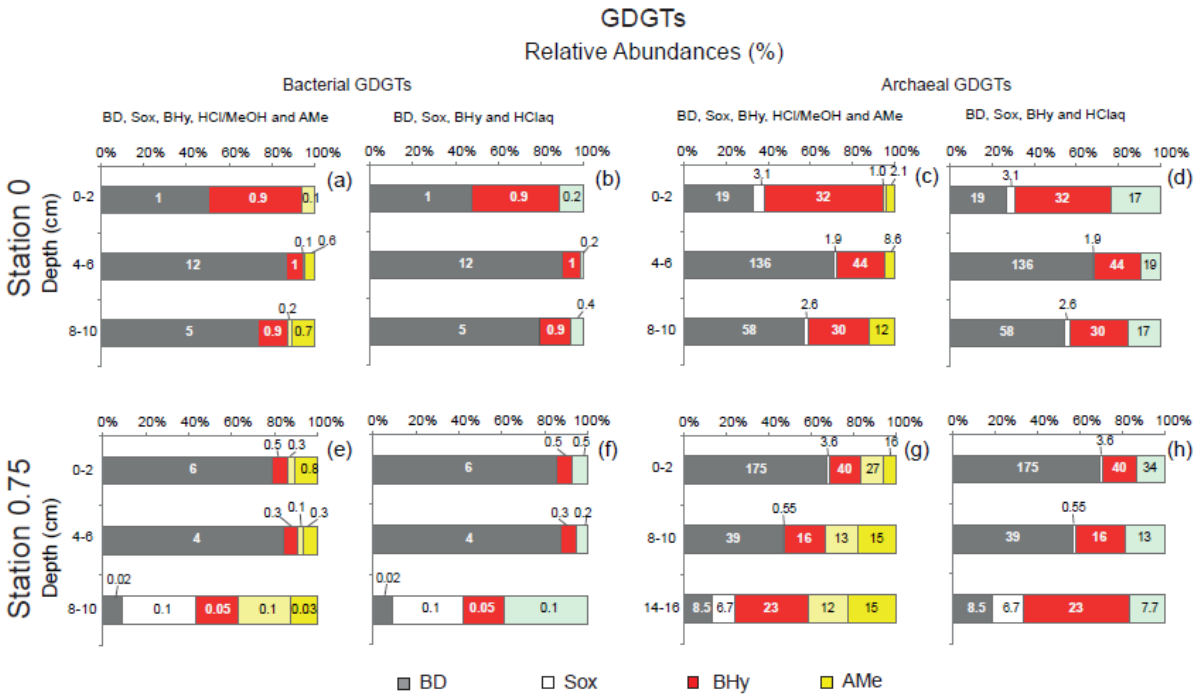

Fig. 5

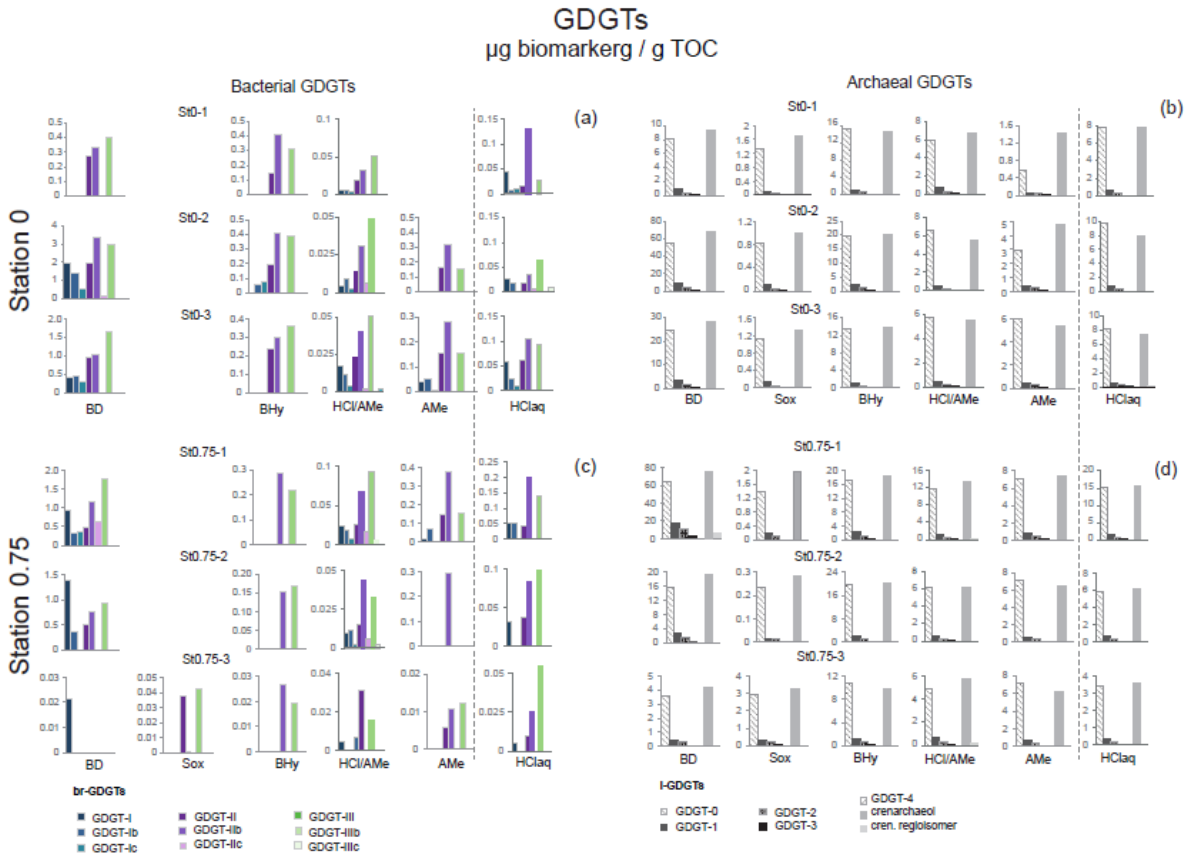

Fig. 6

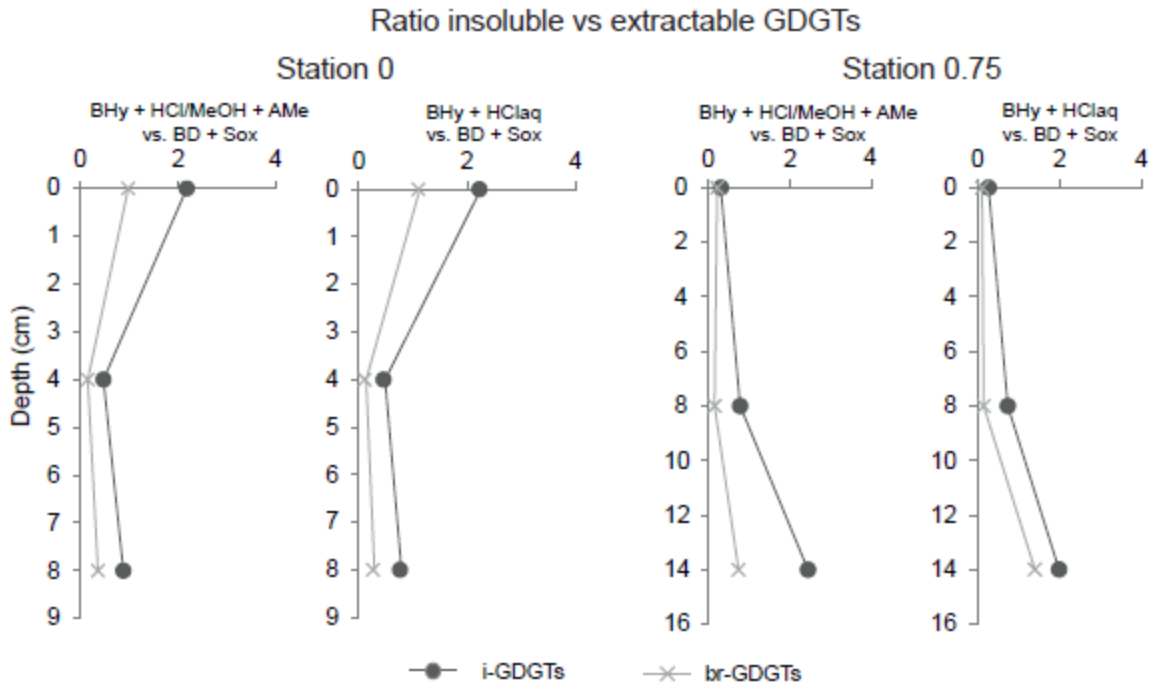

Fig. 7

Table 1. Location, depositional conditions and OC content of ESAO sediments.

	Station 0 (St0)			**Station 0.75 (St0.75)**		
Geographic Coordinates	34.1S 17.5E			34.3S 17.3E		
Water Depth	246 m			1182 m		
Sample code in this work	St0-1	St0-2	St0-3	St0.75-1	St0.75-2	St0.75-3
Sediment depth intervals analysed (cm)	0-2	4-6	8-10	0-2	8-10	14-16
TOC(%)*	0.5	0.6	0.8	1.8	2.2	2.5
TIC(%)*	1.0	1.0	1.3	2.9	3.4	3.4
Oxygen penetration depth (OPD)*	2.89 cm			0.93 cm		
230Th-corrected accumulation rate (vertical flux; Fv)* (g cm^{-2} ky^{-1})	–			~1.87		

** Data from Hernandez-Sanchez et al. (2014a)*

Table 2. GDGT-based proxy values including and excluding insoluble GDGTs and the corresponding reconstructed SST.

Sample	OM pool	TEX_{86}[a]	SST[b]	GDGT index-1[c]	SST[d]	GDGT index-2[e]	SST[f]	BIT
	BD	0.32	2.6	-0.62	5.3	-0.50	4.6	0.067
	Sox	0.38	6.9	-0.42	19	-0.42	10	0
	TE	**0.32**	**2.9**	**-0.60**	**6.7**	**-0.49**	**5.1**	**0.058**
	BHy	0.42	9.6	-0.47	15	-0.37	13	0.030
	HClaq	0.40	7.9	-0.51	12	-0.40	11	0.011
St0-1	HCl/MeOH	0.37	6.0	-0.53	11	-0.43	9.1	0.011
	AMe	0.54	17	-0.36	23	-0.27	20	0
	TI-a	0.41	9.0	-0.49	14	-0.39	12	0.024
	TI-b	0.41	8.7	-0.48	14	-0.39	12	0.023
	TR-a	**0.39**	**7.0**	**-0.52**	**12**	**-0.41**	**10**	**0.035**
	TR-b	**0.38**	**6.8**	**-0.52**	**12**	**-0.42**	**10**	**0.035**
	BD	0.40	8.1	-0.52	12	-0.40	11	0.092
	Sox	0.25	-2.0	-0.67	1.5	-0.60	-2.6	0
	TE	**0.40**	**8.0**	**-0.53**	**11**	**-0.40**	**11**	**0.090**
	BHy	0.37	5.8	-0.53	11	-0.44	8.8	0.028
	HClaq	0.41	8.5	-0.51	12	-0.39	12	0.014
St0-2	HCl/MeOH	0.36	5.0	-0.56	9.1	-0.45	7.9	0.012
	AMe	0.47	13	-0.43	18	-0.33	16	0.062
	TI-a	0.38	6.6	-0.53	11	-0.42	9.7	0.024
	TI-b	0.38	6.7	-0.52	12	-0.42	9.8	0.030
	TR-a	**0.39**	**7.6**	**-0.53**	**11**	**-0.40**	**11**	**0.072**
	TR-b	**0.39**	**7.6**	**-0.52**	**12**	**-0.40**	**11**	**0.073**
	BD	0.39	7.7	-0.53	11	-0.40	11	0.097
	Sox	0.21	-4.5	-0.67	1.4	-0.67	-7.5	0
	TE	**0.39**	**7.2**	**-0.54**	**11**	**-0.41**	**11**	**0.093**
	BHy	0.39	7.2	-0.55	10	-0.41	10	0.042
	HClaq	0.51	16	-0.48	15	-0.29	19	0.028
St0-3	HCl/MeOH	0.35	4.8	-0.55	10	-0.45	7.6	0.016
	AMe	0.47	12	-0.44	17	-0.33	16	0.062
	TI-a	0.43	10	-0.52	12	-0.36	14	0.037
	TI-b	0.40	7.9	-0.52	12	-0.40	11	0.041
	TR-a	**0.41**	**8.4**	**-0.53**	**11**	**-0.39**	**12**	**0.070**
	TR-b	**0.39**	**7.5**	**-0.53**	**11**	**-0.41**	**11**	**0.070**
	BD	0.53	16	-0.46	16	-0.28	20	0.041
	Sox	0.35	4.4	-0.46	16	-0.46	7.1	0
	TE	**0.53**	**16**	**-0.46**	**16**	**-0.36**	**14**	**0.040**
	BHy	0.37	5.9	-0.50	13	-0.43	8.9	0.012
	HClaq	0.39	7.1	-0.49	14	-0.41	10	0.015
St0.75-1	HCl/MeOH	0.40	8.2	-0.48	15	-0.39	12	0.011
	AMe	0.42	9.2	-0.46	16	-0.38	13	0.042
	TI-a	0.38	6.4	-0.49	14	-0.43	9.5	0.013
	TI-b	0.39	7.2	-0.49	14	-0.41	10	0.017
	TR-a	**0.50**	**15**	**-0.46**	**16**	**-0.30**	**18**	**0.032**
	TR-b	**0.50**	**15**	**-0.46**	**16**	**-0.30**	**18**	**0.033**
	BD	0.42	9.5	-0.45	17	-0.37	13	0.13
	Sox	0.48	13	-0.32	25	-0.32	16	0
St0.75-2	**TE**	**0.42**	**9.5**	**-0.45**	**17**	**-0.37**	**13**	**0.13**
	BHy	0.35	4.6	-0.56	8.9	-0.46	7.4	0.022
	HClaq	0.33	3.3	-0.56	9.4	-0.48	5.6	0.026

	HCl/MeOH	0.35	4.5	-0.55	9.6	-0.46	7.2	0.0091
	AMe	0.48	13	-0.44	18	-0.32	16	0
	TI-a	0.34	4.1	-0.56	9.1	-0.47	6.7	0.024
	TI-b	0.39	7.5	-0.51	12	-0.41	11	0.011
	TR-a	**0.39**	**7.6**	**-0.48**	**14**	**-0.40**	**11**	**0.087**
	TR-b	**0.41**	**8.6**	**-0.48**	**15**	**-0.39**	**12**	**0.071**
St0.75-3	BD	0.49	14	-0.36	23	-0.31	18	0.0051
	Sox	0.43	9.9	-0.47	15	-0.37	13	0.024
	TE	**0.47**	**12**	**-0.40**	**20**	**-0.33**	**16**	**0.014**
	BHy	0.41	9.0	-0.47	15	-0.38	12	0.0020
	HClaq	0.42	9.4	-0.52	12	-0.38	13	0.019
	HCl/MeOH	0.48	14	-0.47	15	-0.31	17	0.0047
	AMe	0.42	9.3	-0.45	16	-0.38	13	0.0028
	TI-a	0.42	9.1	-0.48	14	-0.38	13	0.0066
	TI-b	0.43	10	-0.47	15	-0.38	12	0.010
	TR-a	**0.43**	**10**	**-0.45**	**16**	**-0.36**	**14**	**0.0091**
	TR-b	**0.44**	**11**	**-0.45**	**17**	**-0.37**	**13**	**0.011**

a and b after Schouten et al. (2002), Eq. 2 and SST = 0.015 T + 0.28, respectively. SST standard error (s.e.) ±2 ºC

c and d after Kim et al. (2010), Eq. 3 and SST = [67.5 x (GDGT index-1) + 46.9], respectively. SST s.e. = ±4.0 ºC

e and f after Kim et al. (2010) Eq. 4 and [68.4 x (GDGT index-2) + 38.6], respectively. SST s.e. = ± 2.5 ºC

g after Hopmans et al. (2004), Eq. 1

BD Bligh and Dyer extracts

Sox Soxhlet 48 h extracts

TE Total Extractable: Combined BD and Sox
BHy Base Hydrolysis extracts
HClaq Extracts after Carbonate removal with HClaq
HCl/MeOH Extracts after Carbonate removal with HCl/MeOH
AMe Acid Methanolysis extracts
TI-a Total Insoluble: Combined BHy and HClaq
TI-b Total Insoluble: Combined BHy, HCl/MeOH and AMe
TR-a Total Recovered: Combined TE and TI-a
TR-b Total Recoverd: Combined TE and TI-b

Highlights

- 5-80 % of prokaryotic membrane lipids are not solvent-extractable
- 5-50 % of insoluble prokaryotic lipids are released after carbonate dissolution
- BIT index is overestimated when only solvent-extractable GDGTs are considered